

Effect of Progressive Integration of On-Board Systems design discipline in an MDAO framework for aircraft design with different level of systems electrification

Marco Fioriti^{1,*}, Pierluigi Della Vecchia² and Giuseppa Donelli³

¹ Politecnico di Torino (PoliTo), Turin, Italy; marco.fioriti@polito.it

² University of Naples Federico II, Naples, Italy (UniNa); pierluigi.dellavecchia@unina.it

³ German Aerospace Center (DLR), Institute of System Architectures in Aeronautics, Hamburg, Germany; giuseppa.donelli@dlr.de

* Correspondence: marco.fioriti@polito.it

Abstract: The on-board design discipline is sometimes ignored during the first aircraft design iterations. It might be understandable when a single on-board system architecture is considered especially when a conventional architecture is selected. However, seeing the trend towards the systems electrification, multiple architectures can be defined and each one should be evaluated during the first tradeoff studies. In this way, the systems design discipline should be integrated from the first design iterations. This paper deals with a progressive integration of the discipline to examine partial or total effect of the systems design inside a MDAO workflow. The study is carried out from a systems design perspective analyzing the effect of their electrification on aircraft design with different MDAO workflow arrangements. Starting from a non-iterative systems design, other disciplines such as aircraft performance, engine design, aircraft synthesis are gradually added increasing the sensibility of the aircraft design to the different systems architectures. The results show an error of 40% in on-board systems assessment when the discipline is not fully integrated. Finally, using the workflow which allows for greater integration, interesting difference can be noted comparing systems with different level of electrification. A possible mass saving of 2.6% of aircraft MTOM can be reached by properly selecting the systems technologies used.

Keywords: on-board-system design; collaborative MDAO; aircraft design

Citation: Lastname, F.; Lastname, F.; Lastname, F. Title. *Aerospace* **2021**, *8*, x. <https://doi.org/10.3390/xxxxx>

Academic Editor: Firstname Lastname

Received: date

Accepted: date

Published: date

Publisher's Note: MDPI stays neutral with regard to jurisdictional claims in published maps and institutional affiliations.



Copyright: © 2022 by the authors. Submitted for possible open access publication under the terms and conditions of the Creative Commons Attribution (CC BY) license (<https://creativecommons.org/licenses/by/4.0/>).

1. Introduction

The trend towards the On-Board Systems (OBS) electrification is due to different reasons. Firstly, the electrified OBS should reduce the fuel consumption because of their greater efficiency [1,2,3]. This is particularly true when the electrification of the Environmental Control System (ECS) and Ice Protection System (IPS) is considered. In general, all OBS options able to achieve the bleedless engine technology produce beneficial effects on propulsion system efficiency. Secondly, the electrified OBS is more maintainable, testable and their status is easier to monitor positively impacting the operational cost [1,4,5,6]. This is achieved mainly electrifying the Flight Control System (FCS) and Landing Gear System (LGS) avoiding the use of hydraulic technology. The More Electric Aircraft (MEA) and All Electric Aircraft (AEA) initiatives are providing several new OBS architectures with different level of electrification. This greatly differs from few decades ago when only one conventional (i.e. systems using hydraulic and bleed technologies) architecture was considered and the majority of preliminary design models included the OBS as fixed percentage of aircraft mass as first design attempt [7,8,9]. Similarly, nearly all Multidisciplinary Design Analysis and Optimization (MDAO) studies, carried out for aircraft preliminary design, do not involve the OBS discipline focusing on aerodynamics, structural and

engine design [10, 11,12]. This may perhaps be acceptable when facing with conventional OBS architecture assuming mass and volume values supported by statistic equations based on previous products. However, this approximation is not acceptable when MEA and AEA architectures are concerned. Each of those architectures delivers different effects at aircraft level in terms of mass, volume needed and power requirement, to only mention the main parameters affecting the aircraft design. Therefore, consider the electrification trend, the OBS design discipline should be fully included from the first aircraft design iterations evolving together with the other disciplines to obtain a more optimal product.

The integration of the OBS discipline in an MDAO workflow is currently under investigation by some researchers with different approaches [13,14,15]. All of them proposed the integration of OBS design showing the advantages and their complexities, but without comparing the results obtained using the proposed approach with the standard one (i.e. OBS design not integrated). Compared to other studies, the present paper deals with the progressive integration of the OBS design in a distributed MDAO workflow in order to analyze the mutual effects of OBS and aircraft design to understand their actual contributions. In particular, the study permits to better evaluate the OBS architectures with different level of electrification and, at the same time, understand the most appropriate integration depth. In this way, three workflows are proposed, each one with a different integration depth. Four OBS architectures with an increasing use of electrified systems are studied by means of the three workflows. A small regional turboprop aircraft is defined as reference. The electrification of this aircraft category is even more interesting since the trend towards propulsion system electrification.

The present work has been carried out in the frame of the AGILE4.0¹ European research project [16] that has the objective to reduce the time-to-market and the development cost of new products integrating new disciplines to traditional MDAO workflows.

The paper is divided in three main sections. In section III, the reference aircraft and the different OBS architectures are described and increasing electrification level are identified. The three MDAO workflows are described and discussed in section IV. In section V, the results are reported emphasizing the effect on the OBS assessment adding and increasing number of disciplines to the MDA/MDO workflow. Finally, the conclusions have been drawn also highlighting the next expected developments.

2. Reference aircraft and OBS architectures

To perform a quantitative analysis, a reference aircraft has been selected. Considering the interest towards the complete electrification of the small regional turboprop category, an aircraft of this type carrying 19 passengers has been selected. The Top-Level Aircraft Requirements (TLARs), listed in Table 1, show a small transport aircraft able to connect small airports or a small airport with a hub also at large distance. The Maximum TakeOff Mass (MTOM) is limited to 8600 kg to comply with CS23 regulations [17].

Table 1. Reference aircraft TLARs

MTOM	≤ 8600 kg
N. of passengers	19
Maximum Range	1500 km
Speed	0.45 M @ 7620m
Operative Ceiling	7620 m
TOFL	800 m
MTOM	≤ 8600 kg

¹ AGILE4.0 research project. Retrived 29/01/2022 online: website: <https://www.agile4.eu/>.

Among the several possible OBS architectures that could be defined, four of the more promising have been considered for this kind of aircraft. Each of them has a different electrification level and has been defined starting from a different aim. The electrification level L_E is here defined as the ratio of the non-propulsive power produced by the electric system P_E and the total non-propulsive power P_T [18]:

$$L_E = \frac{P_E}{P_T} \quad (1)$$

The L_E is a parameter that assumes values always between 0 and 1.

The first architecture considered is the conventional one depicted in Figure 1(a). It represents the standard OBS arrangement for a turboprop aircraft and it has the lowest value of L_E . Three different kinds of power are generated and distributed, they are the electric, hydraulic, and pneumatic power. The Electrical Power Generation and Distribution System (EPGDS) consists by two redundant lanes. The electric power is generated by two 28 VDC starter generators (one per engine) and distributed by two PPDU (Primary Power Distribution Units) that supplies all the main electric utilities. Two inverters supply a double 115 VAC bus for some avionic equipment and some part of the IPS by means of SPDU (Secondary Power Distribution Units). The electric system supplies the fuel system, the avionics, the lights and furnishing, and part of the IPS (i.e. probes, sensors, propellers leading edges). The Hydraulic Power Generation and Distribution System (HPGDS) comprises two lanes powered by two Engine Driven Pumps (EDP) rated at 20.7 MPa. The HPGDS supplies the landing gear and the flap actuators. Finally, the pneumatic power is provided by the engines bleed system rated at 5 bar. The pneumatic power is supplied to the ECS and part of the IPS. In particular, the pneumatic power is used by wing and tail IPS to inflate and deflate the leading-edge boots. It is worth noting the FCS (apart from the flap) for this aircraft category relies on pilots' force and the control surfaces are mechanically connected with the pilots' controls.

The first example of MEA architecture, called MEA1, is depicted in Figure 1(b). Compared to the conventional architecture, the HPGDS is completely removed. The flap actuators are replaced by Electro Hydrostatic Actuators (EHA). In the same way, the actuators of the braking, steering and retracting systems of the landing gear are EHA. Usually, the EHA need to be supplied by high voltage 270 VDC power bus. For this reason and to reduce the mass of the electric system, the EPGDS of the MEA1 architecture consists of two 270 VDC busses and two 28 VDC busses. The high voltage busses supplied the greater part of the utility systems, whereas the avionic system is connected to the low voltage busses. Two high voltage starter generators power the EPGDS main busses, and two DC-DC converters provide power to the low voltage bus. No changes are made to the pneumatic system which still relies on engine bleed system. Since the power required by flap and landing gear is quite restrained and not continuous, the MEA1 architecture fairly increases the L_E . Its main advantage is to reduce the overall mass of the OBS by completely removal of the HPGDS.

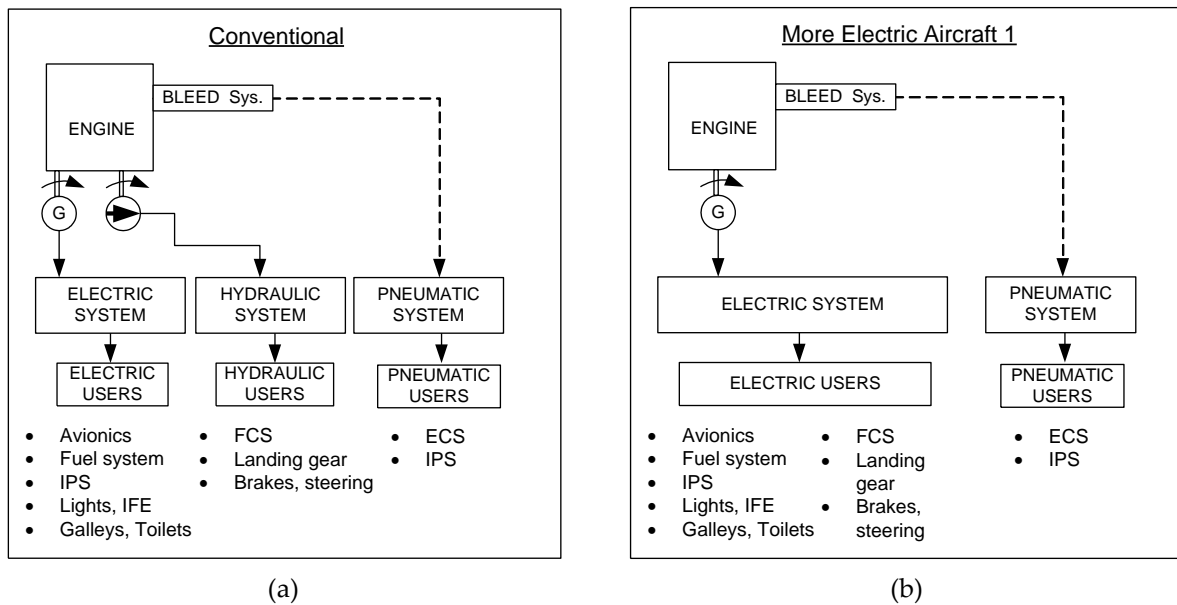


Figure 1. Conventional (a) and more electric n.1 (b) OBS architectures.

126

Conversely, the second MEA architecture (Figure 2(a)), here called MEA2, aims more at increasing the L_{E^*} to optimize the power consumption, than to achieve a mass saving. The main difference, compared to the conventional architecture, is the removal of the engine bleed system. The pneumatic power is generated by a series of centrifugal compressors arranged in two lanes for redundancy. The compressors are driven by electric motors connected to the EPGDS. Thus, the pneumatic power generation is completely electrified allowing for the bleed-less technology.

127

128

129

130

131

132

133

134

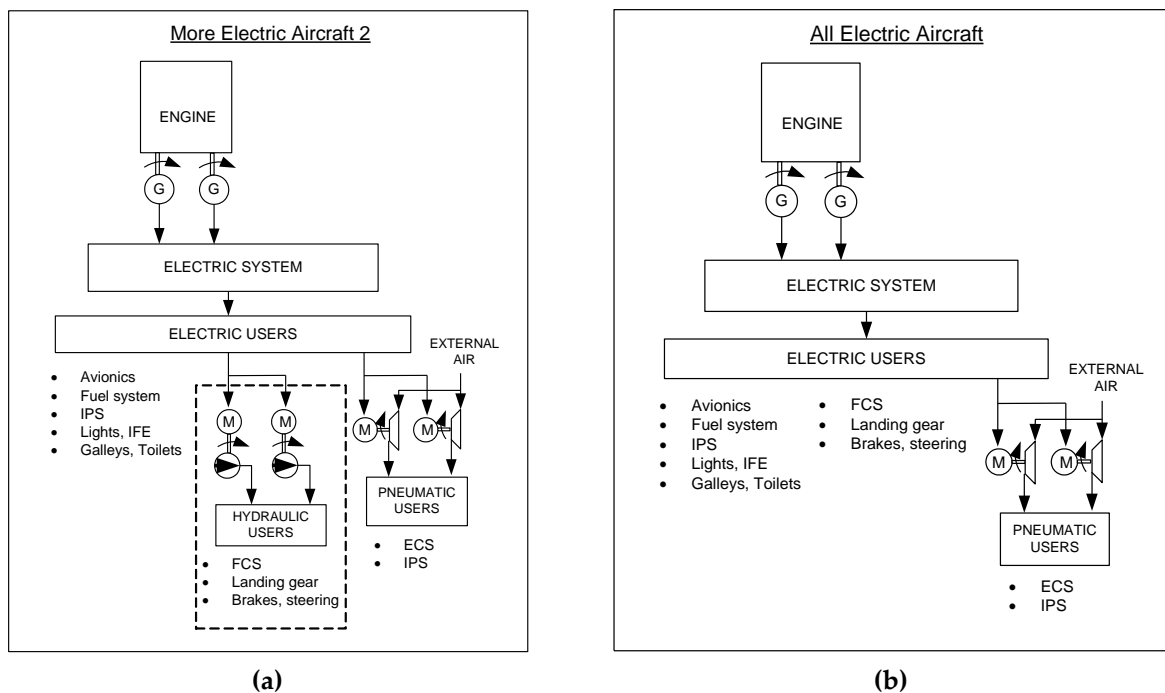


Figure 2. More electric n.2 and all electric OBS architectures.

135

The electrified pneumatic system is still used to provide power to the ECS. The IPS, that in the conventional architecture was a pneumatic user of the engine bleed system, now relies in the electric pneumatic system. Due to the high electric power demanded by

136

137

138

both ECS and IPS, the EPGDS uses the same architecture of the MEA1 with a high voltage (i.e. 270 VDC) busses and starter-generators. Finally, the HPGDS is not removed but it is an electric user due to the use of Motor Driven Pumps (MDP) instead of EDP.

Finally, the AEA architecture depicted in Figure 2 (b) includes the electrified systems of both MEA1 and MEA2 architectures. Consequently, AEA reaches the greater L_E since all systems are powered by means of the EPGDS, no hydraulic neither pneumatic power is directly required. This is achieved removing the hydraulic actuation system and opting for high voltage EHAs. The ECS and IPS are connected to the electrified pneumatic system avoiding the need of any engine bleed system. All the mentioned systems plus the engine starting system are directly connected to the 270 VDC bus of the EPGDS. Only the avionics and some other small users need a DC-DC converter to be supplied by means of the low voltage bus (28 VDC).

3. Implementation of the design workflows

To investigate the effect on global and systems results when the OBS discipline is not integrated or it is partially and fully integrated, three different MDAO workflows are here proposed. Each workflow is defined within the RCE environment² and connects tools coming and stored in different universities and research centers. The tools are connected to each other by means of an *.xml* file called CPACS³ already modified in previous research activities [18] to be compatible with OBS integration.

3.1. Disciplinary competences

The disciplinary competences included in the workflows are described in this section.

3.1.1. OpenAD

OpenAD is an overall aircraft conceptual design tool that aims at providing a multi-disciplinary and multi-fidelity design environment for aircraft design to evaluate and assess various concepts and technologies at aircraft level [19,20,18]. It is based on the well-understood and mostly publicly available handbook methods⁴ [22,23,24,25,26,27] and on own methods for disciplines for which no adequate or only insufficient methods could be sourced from the literature [28]. OpenAD, programmed object oriented in the Python scripting language, is a key enabler tool to generate a consistent initial evaluation of an air vehicle design. The current design space is valid for aircraft from commuter aircraft (e.g. Dornier 228) up to 800 passengers (e.g. A380) with enhanced capabilities on the design and thermodynamic cycle calculation of turbofan and turboprop engines. Dedicated to tube and wing concepts, the software offers wide capabilities to design, among others, strut braced wings, canards, fuselage mounted engines and any combination. To achieve a consistent design, a minimum set of top-level aircraft requirements (TLARs) and design parameters have to be set. Focusing on the TLARs, it is mandatory to assign the design range, the cruise altitude, the Mach number, the payload, the reserve mission, the take-off field length and the landing field length. Instead, within the design parameters, decisions related to configuration of the aircraft components have to be made. For example, for the initial sizing, the design parameters for wing loading and thrust-to-weight ratio are usually specified or varied as a design of experiment or optimization target among others. In case that no decisions are made, OpenAD is set to design as default a conventional aircraft configuration as the Airbus A320 or the Boeing 737. However, calibration factors and design constraints can be defined in the tool input to design new aircraft configuration. In

² Remote Control Environment (RCE). Retrieved 29/01/2022 online, website: <https://rcenvironment.de/>.

³ Common Language for Aircraft Design (CPACS). Retrieved 29/01/2022 online, website: <http://cpacs.de/>.

⁴ Luftfahrttechnisches Handbuch (2022, 01 15). Retrieved 01/15/2022 online, website: <https://www.lth-online.de/>.

this case, the masses, center of gravity and geometry of each component will be adjusted due to the set-up parametrization. Concluding, starting from TLARs and design parameters, OpenAD generates a CPACS output file where the relevant aircraft data are exported according to the CPACS schema. Instead, additional output can be stored into the tool specifics.

3.1.2. ASTRID

ASTRID is a tool dedicated to OBS design and it has been developed at Politecnico di Torino [29]. As depicted in Figure 3, it is composed by the aircraft conceptual design and OBS design modules. The first module was not used since the conceptual design results are already available from OpenAD. Starting from the main aircraft masses, dimensions and performance and additional information at OBS level (e.g. desired architecture, bus voltages, hydraulic system pressure etc.) ASTRID calculates the loads and functions that each utility system must satisfy. The design of the utility systems (i.e. FCS, ECS, LGS, avionics etc.) is carried out for each phase of the mission profile delivering systems mass, dimensions and power required. The power requirements are then used to design the electric, pneumatic, and hydraulic power generation and distribution systems. Finally, the mass of all OBS, their volumes and the global engine offtakes are obtained.

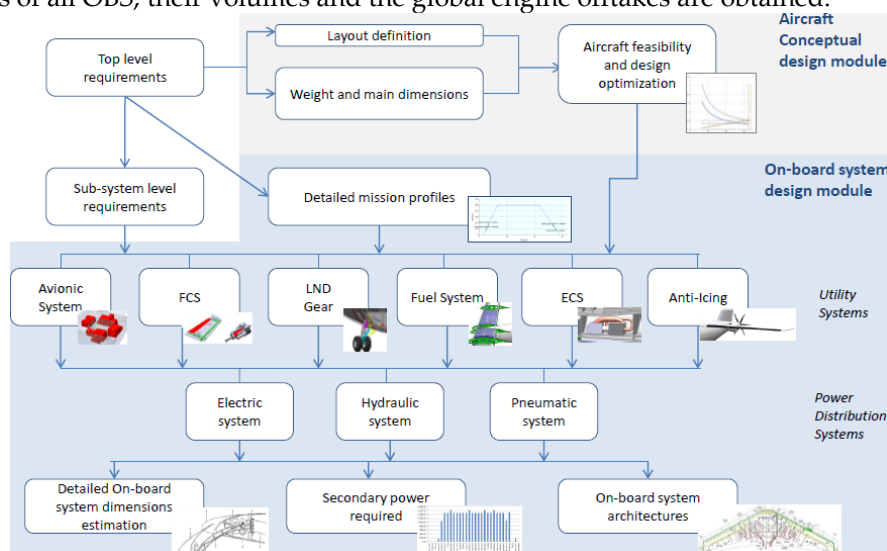


Figure 3. ASTRID OBS design process.

These results are obtained at main equipment level and for each phase of the mission. The tool is able to design standard and different type of MEA and AEA architectures.

3.1.2. Performance

Aircraft performance tool is a simulation-based software which allows whole aircraft on-ground and in-flight calculation, including cruise, take-off, landing, climb, block fuel and time, and emissions performance. It uses a set of functionalities of JPAD library [30,31,32,33] (Java Programming for Aircraft Design), an object-oriented API suitable for aircraft design, analysis, and optimization whose core-pattern is depicted in Figure 4.

The input data needed are referred to the required characteristics (aircraft drag, at least in clean, take-off and landing conditions), the available characteristics (installed thrust, fuel consumption and emission indices, at different flight ratings, altitude, and Mach number), the lift characteristics (at least in clean, take-off and landing conditions) and the design weights (at least maximum take-off).

The take-off calculation module computes all the take-off performance using a simulation-based approach as stated in [31,32,33]. The analysis procedure expects to solve an appropriate set of Ordinary Differential Equations (ODE), which describes the aircraft equations of motion during all the take-off phase up to the obstacle. Balanced field length is computed in case of OEI (one engine out condition). Here the accelerate go and

accelerate stop distances are simultaneously computed (solving similar ODE systems) and balanced field length obtained where these distances are equal.

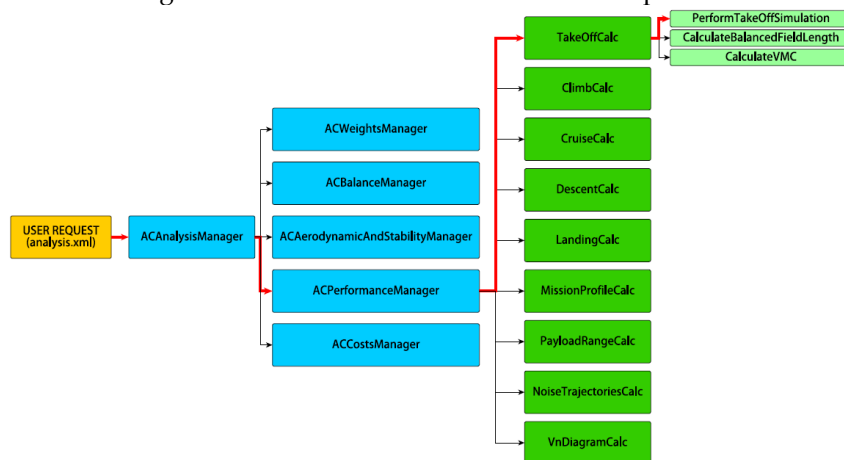


Figure 4. JPAD core-manager calculator pattern – Example of Take-off performance, courtesy of Trifari[33].

Similar to the take-off, also for the landing phase a simulation-based approach, involving the resolution of an ODE system, is used. The simulation starting point is assumed at 1500ft above runway and a stabilized approach with a constant flight path angle and calibrated airspeed are maintained up to obstacle height over the runway. From the landing obstacle altitude (50ft) the aircraft begins the final approach down to the initial flare rotation. During the flare rotation a smooth transition from a normal approach attitude to a landing attitude must be accomplished by gradually rounding out the flightpath to one that is parallel with, and within a very few inches above, the runway. During this rotation the angle of attack increases providing for higher lift as well as induced drag resulting in a deceleration of the aircraft. At the end the aircraft must touch the ground with its main landing gears and a with a reasonably low value of the vertical speed. After the touch-down, after few seconds of wheel free-roll, the pilot must apply a breaking action of all wheels brakes, deflect all spoilers and set each engine setting to ground idle. The simulation ends when the aircraft speed reaches a value of zero.

Climb performance are computed for twofold reason: the first is to evaluate the best climb performance of given aircraft (rate of climb, glide ratio, ceiling in AEO and OEI conditions); the second to exactly compute the mission parameters (fuel consumed, range and time). In the second mode, the calibrated airspeed CAS, the aircraft rate-of-climb ROC and initial cruise altitude must be specified, and, if not reachable, the tool switch to best rate of climb condition and practical ceiling altitude.

Cruise performances are computed to evaluate aircraft flight envelope and mission profile cruise segment (fuel flow and distance covered). In the second case, the cruise altitude, the desired Mach number, and cruise mode must be specified (fixed or variable altitude). If some parameters are violated, the tool compute cruise performance at cruise ceiling altitude and maximum achievable Mach number.

From prescribed final cruise altitude, descent performance is computed to evaluate the fuel flow and range of descent phase. CAS airspeed and rate-of-descent (ROD) must be prescribed, and, if violated, the tool uses the minimum ROD condition.

Block fuel, block range and block time data are computed iterating take-off, climb, cruise, descent, and landing segments coherently to the prescribed input data described before (altitude, speeds, ROC, ROD, etc.). In the design mode the tool is also capable to add eventual alternate, loiter, reserve phases. A schema of the mission profile analysis is shown in Figure 5, highlighting the inner loops to converge on required specifications. The main objective is an accurate calculation of block fuel, time, and emissions.

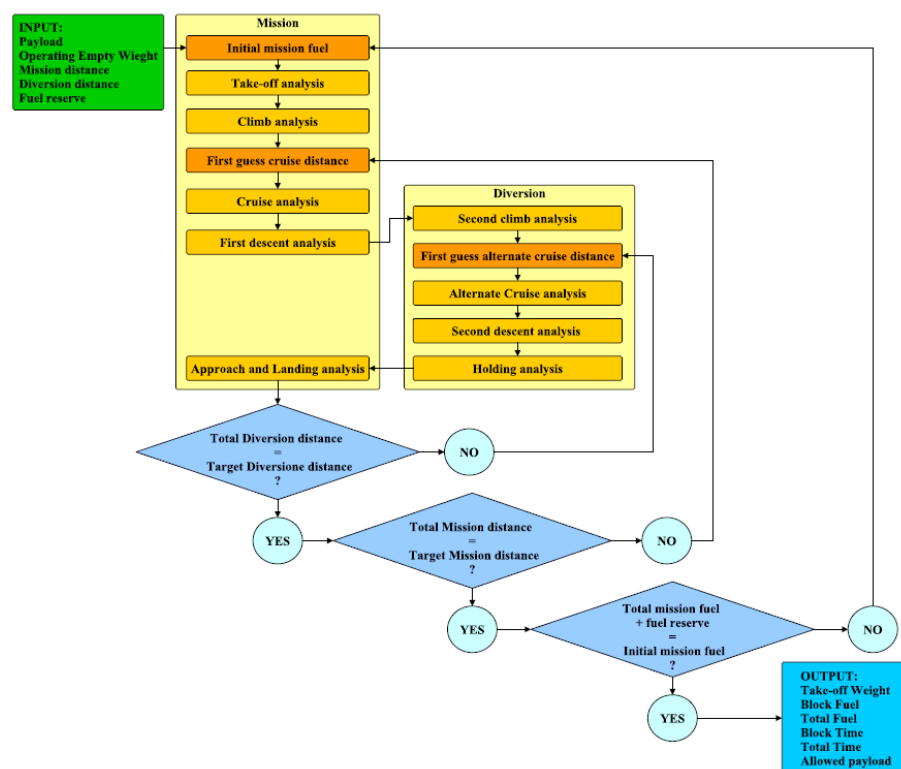


Figure 5. Flowchart of the mission profile analysis performed by JPAD, courtesy of Trifari[33].

3.1.3. Engine

Engine modelling is crucial for performance evaluation. The Engine tool is suitable to design an engine deck, providing thrust or power characteristics, fuel consumption, emissions indices, masses and geometry. The tool needs as inputs required thrust for several ratings (TopOfClimb, TakeOff, Cruise), engine type (turbofan, turboprop) and provide as output the engine maps, in terms of Thrust versus Mach, Altitude, throttle ratings and temperature condition. These maps are obtained with GASTURB⁵ software. The tool is also able to rubberize the designed engine, in a range of $\pm 20\%$ of maximum thrust or power. Finally, the tool also provides estimation of engine dry mass and main geometrical characteristics.

3.1.4. SFC_sensitivity

Tool provided by Politecnico di Torino, it is capable to calculate the effect of power offtakes on engine Specific Fuel Consumption (SFC). It is based on a scalable engine deck of turboprop engines. The main inputs are the basic SFC provided by the engine design tool and the power offtakes and air-bleed requirements provided by ASTRID tool. The basic SFC is used as reference point to generate a new SFC value collecting the adverse effects of providing additional mechanical power and compressed air required by OBS. The tool is able to differentiate among the increase of SFC due to power offtakes and due to bleed requirements. Therefore, the tool can be used to evaluate the different OBS architectures that have a different balancing of required mechanical power and bleed air.

3.1.5 Aircraft Synthesis.

As widely explained above, OpenAD is a software tool for preliminary aircraft design used to generate a CPACS output file, including the relevant data of an aircraft, starting from TLARs and design parameters. Nevertheless, distributed collaborative design workflows usually include analysis capabilities of different levels of modelling fidelity. These

⁵ [Online]. Available: <https://www.gasturb.de/index.php>. [Zugriff am 18 October 2021].

broader design environments required not only a provider of initial solutions but also a tool able to dynamically adapt to the results provided by the disciplinary tools, performing the required synthesis calculations. OpenAD is an essential part of the multidisciplinary and multi-fidelity design workflow since it is used to derive an initial design as well as to synthesize higher fidelity disciplinary results into the design. Differently from the OpenAD initializer, in this case the main inputs for Open AD are the design parameters estimated by other high-fidelity tools. A CPACS output file, assessed on these new design parameters values, is the main output of the OpenAD aircraft synthesis.

3.2. Analysis Workflow definition

After the description of the tools involved is now possible to define the workflows proposed. Each of them represents a different level of OBS integration. From their results, it is possible to understand the effects, at aircraft design level, of the OBS integration and systems electrification.

3.2.1 Workflow 1

The first workflow tested (see Figure 6) represents a simple connection of the aircraft conceptual design discipline (i.e. OpenAD tool) with the OBS design (i.e. ASTRID tool). Here, the OBS masses assumed in conceptual design phase by means of percentages of Operating Empty Mass (OEM) are overwritten with the results coming from a preliminary design of the OBS. No converging loop is here considered, therefore the snowball effect is not taken into account. However, the aircraft global masses have been made consistent after ASTRID calculation. Without the presence of a converging loop and recalculation of the aircraft performance and masses, this basic workflow can be considered as a reference of an aircraft design where the OBS discipline is executed but not actually integrated. The only integration is represented, as depicted in Figure 6, by great number of parameters regarding aircraft geometry, mass and performance used as input for the OBS preliminary design.

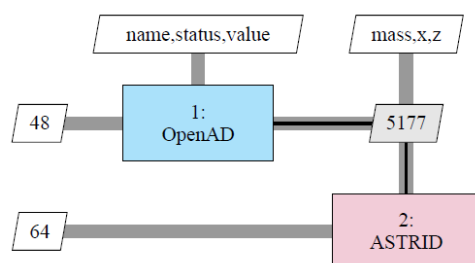


Figure 6. First workflow tested – OBS not integrated

3.2.2 Workflow 2

The second workflow (see Figure 7) represents a partial integration of the OBS discipline in the whole aircraft design. The aircraft conceptual design module (i.e. OpenAD) is used to initialize the converged MDA. After the OBS preliminary design, two other tools are employed to calculate the performance and to design the engine with a greater fidelity compared to the conceptual design. Moreover, these two additional tools are initialized with the new aircraft masses that consider the OBS masses coming from ASTRID. After the calculation of flight performance and the engine mass and geometry, the MDA is reiterated until MTOM convergency. This represents a first example of OBS integration that is focused only on mass parameters. This means that the effect produced by the OBS masses is considered by the new masses of the engine and on aircraft performance (i.e. fuel mass).

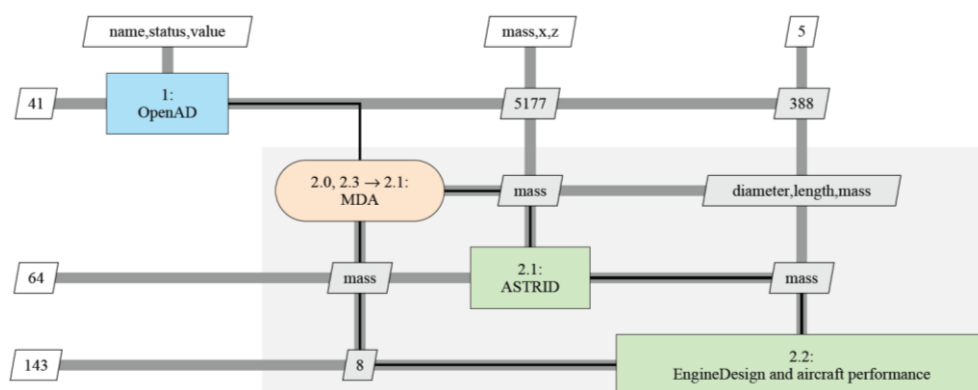


Figure 7. Second workflow tested – OBS partially integrated

3.2.3 Workflow 3

In the third workflow proposed (see Figure 8) the SFC sensitivity tool is added. This tool is included inside the MDA convergency loop and executed after the engine design. An important variable of OBS architectures is the power requirement. The SFC sensitivity tool is able to define a new engine SFC depending on systems power offtakes and bleed air required. Since the systems power requirement changes during the mission, for each mission phase a new SFC is provided. Following the workflow implementation and additionally to the second workflow, the OBS design also provides power requirements for each mission phase. The SFC sensitivity tool modify accordingly the engine SFC used in both performance and engine design tools. In this way, the additional fuel burnt due to OBS power requirement and the secondary effect of reducing engine efficiency (i.e. increasing engine SFC) is taken into account during mission performance calculation.

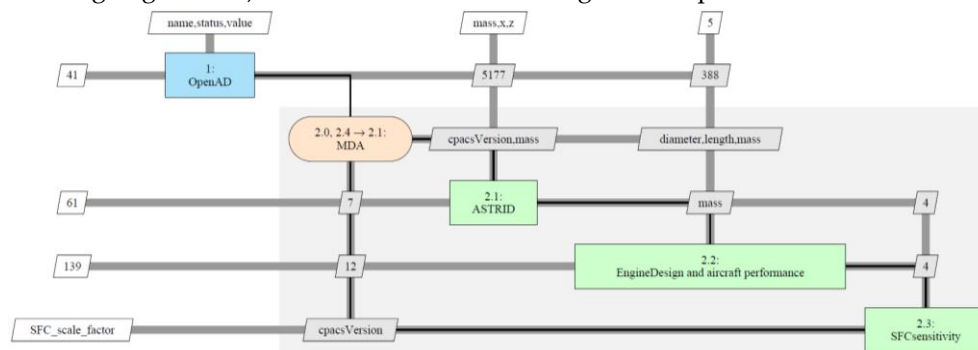


Figure 8. Third workflow tested – OBS partially integrated

3.2.4 Workflow 4

Lastly, in the fourth and final workflow depicted in Figure 9, the aircraft airframe and geometry redesign is added in the MDA converging loop. Therefore, the Aircraft Synthesis tool enables the full integration of the OBS discipline allowing for the complete snowball effect of the aircraft masses. From the OBS design prospective, this workflow allows to quantify the influence of the different architectures on the airframe and engine mass and on aircraft performance. Also, the influence on the fuel consumption is fully considered quantifying both the mass variation due to a different aircraft mass and a different effect on engine SFC. It is worth noting that changing the OBS architecture, the small masses variation is propagated at aircraft level redesigning it. Therefore, for each architecture a slightly different aircraft is obtained. However, each of them is compliant with the TLARs listed in Table 1.

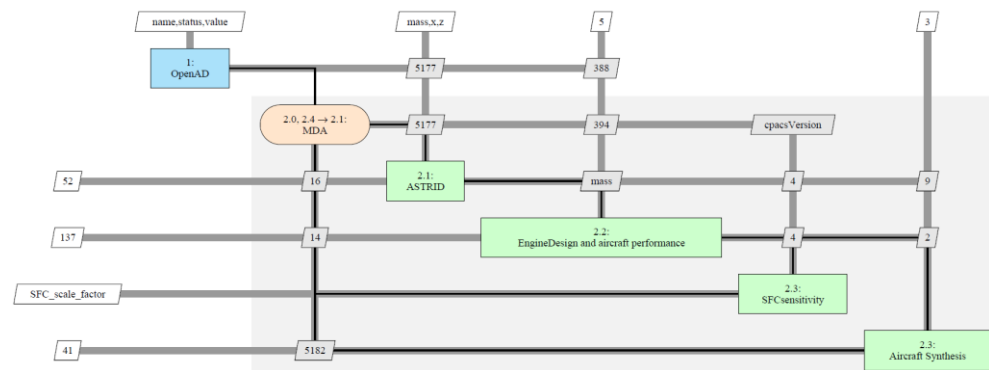


Figure 9. Fourth workflow tested – OBS fully integrated

4. Results and discussions

Before focusing on the different results obtained running the different workflows, the results of OAD and performance are showed. The multi-disciplinary and multi-fidelity workflow starts with OpenAD, the conceptual aircraft design tool. It is used to obtain the reference aircraft baseline, thus all the main aircraft data, starting from the TLARs.

4.1. Reference aircraft

The reference aircraft is a small regional turboprop aircraft, carrying 19 passengers from airports with relatively short runways (TOFL of 800 m), flying with a speed cruise of 0.45 Mach at 7620 m. It can be used to connect small airports to each other or to hub, also at large distance having a range of 1500 km. These TLARs, summarized in Table 1, are the inputs needed from OpenAD to run. However, other configurational decisions must be taken on some design parameters to obtain the desired baseline. The vertical position of the wing with respect to the fuselage and the engines allocation are some of them. In fact, as default, OpenAD is set to design a conventional aircraft configuration like the Airbus A320 or the Boeing 737. However, differently from them, for this reference aircraft a high-wing layout has been adopted for similarity with other 19-pax aircraft configuration, i.e. the Dornier 228. In addition, the relative engines x-position with respect to the wing is set to zero. In this way, engines are directly mounted under the wing, not having the need for pylons. The fuselage layout, chosen elliptical, is another additional design parameter provided as input to OpenAD.

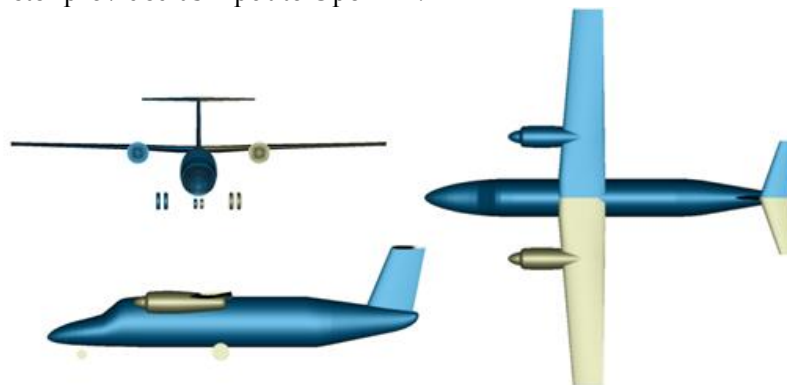


Figure 10. Three views of the reference aircraft.

The reason of this choice relays in the need for pressurization due to the altitude at which the aircraft must fly. This aspect differentiates this reference aircraft to other 19-pax aircraft configurations, like Dornier 228 or Beechcraft 1900, usually flying at lower altitude, and thus characterized by square fuselage layout. Moreover, slats and spoilers have been not included in the OpenAD inputs since these components are usually not adopted by 19-pax aircraft configurations. Providing as input the TALRs and the specified

additional design parameters, OpenAD generates the reference aircraft baseline whose three-views are shown in **Figure 10**. Some representative aircraft specifications are instead reported in Table 2. As required, this aircraft is compliant with the C23 showing a MTOM of about 8.5 tons.

Table 2. Specification of the reference aircraft.

Specifications	Value	Unit
N pax	19	-
Mass per pax	93	kg
Max Payload	2052	kg
Design Range	650	nm
Design Payload	1976	kg
Design Cruise Mach	0.45	-
sTOFL	800	m
Cruise Altitude	7620	m
N Pilots	2	-
MTOM	8478	kg
OEM	5442	kg
MZFW	7495	kg

The results of OAD are also confirmed and refined by the performance tool. From the flight envelope depicted in Figure 11(a), it is worth noting the aircraft reaches (and slightly exceed) the required speed at ceiling altitude. This is the design point for the propulsion system. For this reason, as shows in Figure 11(b), the aircraft outperform the take-off field length requirement. Therefore, the engines could be flat rated for ground operation. Moreover, the speed requirement lead to a greater real ceiling altitude as depicted in Figure 12(a). However, as for other aircraft (e.g. Beechcraft 1900d), the maximum ceiling is limited by the cabin pressurization at 7600m. This decrease the fuselage mass since there is no need for this kind of aircraft to flight at higher altitude. Finally, Figure 12(b) shows the aircraft meet the maximum range requirement of 1200 km.

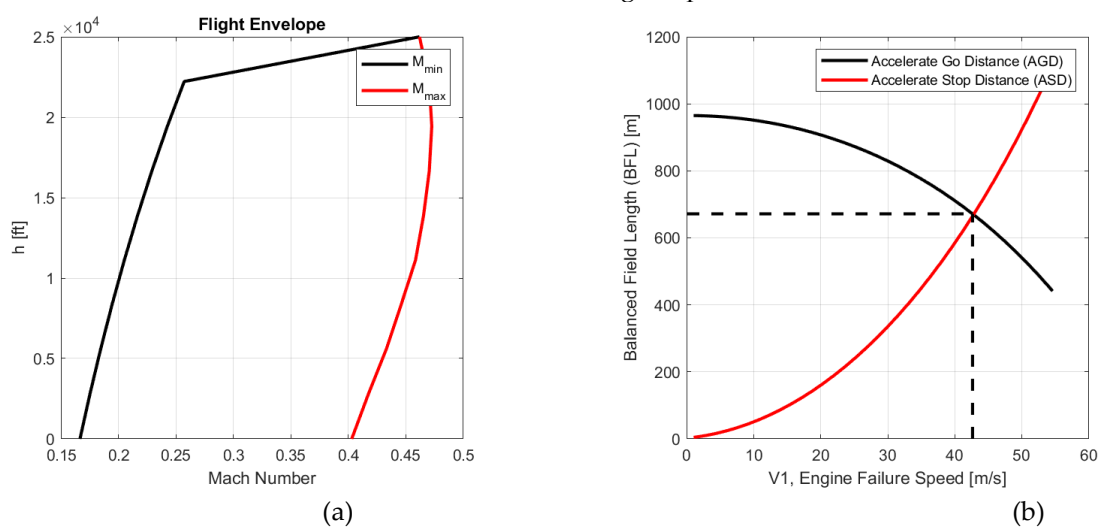


Figure 11. (a) Aircraft envelope and (b) balanced field length.

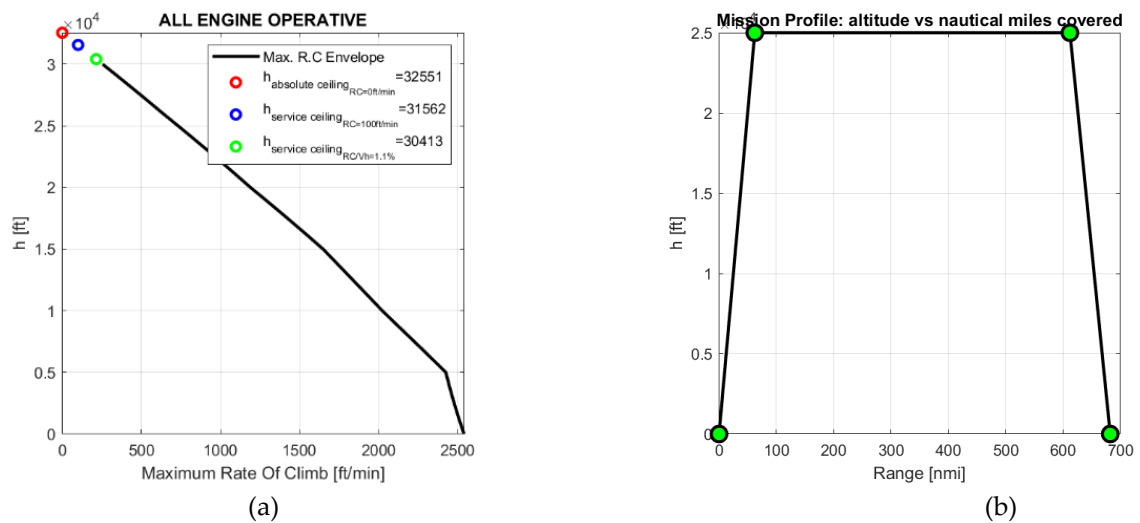


Figure 12. (a) Rate of climb and (b) mission profile.

4.1. Workflow's comparisons

The main results are summarized in terms of aircraft masses and the OBS masses in Table 3 individually for each of the four workflows. Moreover, for each workflow, four columns are defined to list the results of the four OBS architectures. In this way, it is possible to investigate both the effect of systems electrification and the different results obtained increasing the integration of the OBS design with the other disciplines. It is worth noting, the OBS masses change with the architecture, but they are practically constant with the integration level. This means that the OBS is certainly sensitive to its architecture, but a smaller effect is inherited from the other disciplines since the aircraft TLARs remain constant. Focusing on OBS masses in all the workflows it is possible to note:

- The mass of the systems that do not participate to the electrification (e.g. avionics, furnishing, fire protection, oxygen and lights) remain constant.
- The electrification of the actuation system of the flight control and landing gear slightly increase the mass of these system since the greater mass of the EHAs compared to hydraulic actuators.
- An increase of the mass of ECS and IPS can be noticed for the electrified architecture. This is mainly due to the use of additional components (i.e. electric motor compressors).
- The electrification only partially increases the EPGDS mass since the use of high voltage components partially dampen the increase of mass due to the use of more powerful components.
- The main advantage of the electrified architectures is given by the removal of the HPGDS and/or the PPGDS that always produce a reduction of the total systems mass.
- Finally, the OBS electrification always produces a beneficial effect in terms of mass reduction. MEA1 is lightest architecture followed by the AEA and MEA2.

Considering now the results at aircraft level, it can be noticed a variation when comparing the architectures and the different workflows. Since the rationale is different for the two variations, they are addressed separately. At first, the different influence of the OBS electrification on the entire aircraft is explained, then the changes in the global results for each workflow is addressed. To explain the influence of the OBS electrification is more convenient to focus on the results of the fourth workflow that is able to catch all the OBS influences to the overall aircraft design.

Table 3. Results of the three MDA workflow

436

Masses (kg)	Workflow n.1				Workflow n.2				Workflow n.3				Workflow n.4			
	Conv	MEA1	MEA2	AEA	Conv	MEA1	MEA2	AEA	Conv	MEA1	MEA2	AEA	Conv	MEA1	MEA2	AEA
MTOM	8630	8470	8564	8495	8633	8456	8563	8484	8619	8438	8530	8452	8620	8394	8511	8413
ZFW	7647	7486	7580	7511	7633	7464	7565	7491	7563	7391	7490	7416	7660	7454	7570	7482
OEM	5595	5434	5528	5459	5581	5413	5513	5439	5587	5415	5514	5440	5608	5402	5518	5430
Airframe	n.a.	n.a.	n.a.	n.a.	n.a.	n.a.	n.a.	n.a.	n.a.	n.a.	n.a.	n.a.	2356	2326	2342	2328
M_FUEL	n.a.	n.a.	n.a.	n.a.	1058	1049	1055	1050	1056	1046	1040	1036	1063	1042	1043	1033
Operator items	468	468	468	468	468	468	468	468	468	468	468	468	468	468	468	468
Tot sys + Operator items	2108	1948	2041	1973	2100	1930	2029	1956	2100	1930	2029	1956	2101	1927	2028	1953
Avionics	135	135	135	135	135	135	135	135	135	135	135	135	135	135	135	135
FCS	141	144	141	144	142	144	141	144	142	144	141	144	142	143	141	143
IPS	68	68	72	72	68	68	72	72	68	68	72	72	69	68	72	72
ECS	107	107	129	129	107	107	129	129	107	107	129	129	107	107	129	129
Fuel systems	55	55	55	55	40	40	39	39	40	40	39	39	40	40	40	39
LNDG	332	354	332	354	337	353	334	353	337	353	334	353	337	351	333	352
Furnishing	820	820	820	820	821	819	820	820	821	819	820	820	821	819	820	819
Fire protection	10	10	10	10	10	10	10	10	10	10	10	10	10	10	10	10
Lights	68	68	68	68	68	68	68	68	68	68	68	68	68	68	68	68
Oxygen	24	24	24	24	24	24	24	24	24	24	24	24	24	24	24	24
Water Waste	0	0	0	0	0	0	0	0	0	0	0	0	0	0	0	0
APU	0	0	0	0	0	0	0	0	0	0	0	0	0	0	0	0
PPGDS	56	56	0	0	56	56	0	0	56	56	0	0	56	56	0	0
HPGDS	99	0	94	0	99	0	94	0	99	0	94	0	99	0	94	0
EPGDS	194	107	163	163	194	107	163	163	194	107	163	163	194	107	163	163

437

In **Figure 13** these results are depicted in terms of comparison of the electrified architectures with the conventional one. The following consideration can be drawn:

- Due to the completely removal of the HPGDS the MEA1 and the AEA achieve a reduction of systems mass of about respectively 8 and 7%;
- AEA architecture is able to reach the highest fuel mass saving (2.8%) summing up two contributions: MTOM reduction due to OBS mass reduction and engine SFC enhancement due to the use of the bleedless technology. It is worth noting that MEA1 and MEA2 enable the same two contributions but separately. The reduction of fuel mass, for MEA1 (2.0%), is only due to the lighter OBS whereas, for MEA2, the fuel reduction (1.9%) is mainly due to the use of bleedless technology. The effect of the two contributions on fuel saving is not linear and the overall effect cannot be represented by a simple sum of the individual contributions.
- Considering the mass distribution for this kind of aircraft, the mass saving obtained electrifying the OBS is dampened for the other aircraft components (e.g. airframe mass) and for the whole aircraft (e.g. OEM, MTOM, etc.). For example, the OBS mass saving of 8.3% achieved by MEA1 produce a MTOM reduction of 2.6%.
- Finally, considering the reduction of MTOM, the advantage obtained by adopting MEA1 and AEA architectures is similar. MEA2 is only able to achieve the half of mass saving of the other electrified OBS.

438

439

440

441

442

443

444

445

446

447

448

449

450

451

452

453

454

455

456

It is worth noting that the advantage of using the bleedless engine technology employed in MEA2 and AEA is strongly connected with the aircraft mission duration. The reduction of engine SFC could produce a greater fuel reduction in long haul aircraft entailing a bigger MTOM saving [18]. Therefore, the results here presented are dependent on the aircraft category.

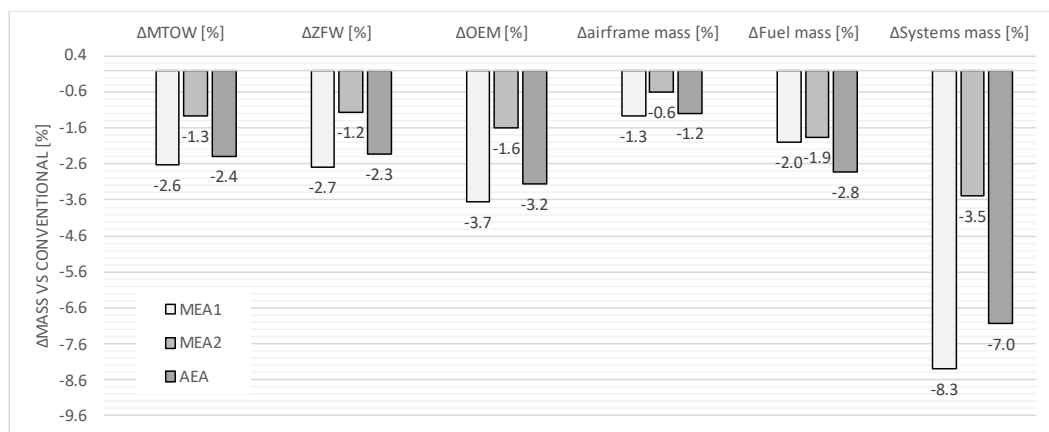
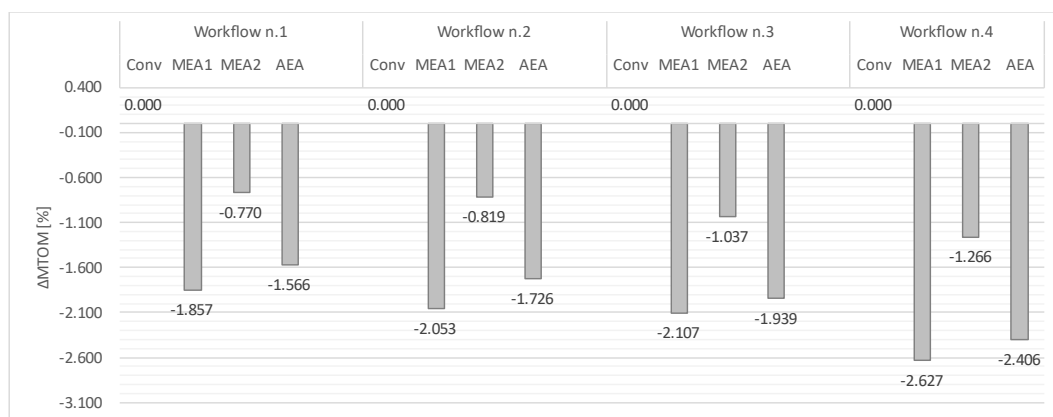


Figure 13. Comparison between conventional architecture and MEA1, MEA2 and AEA (results from workflow n.4)

A second important achievement is the variation of the results by changing the OBS integration with the other design disciplines. In this way, it is now possible to quantify the possible error in evaluating different OBS architecture with disciplines with inadequate integration between them. From Figure 14, it is possible to see the increasing difference, in terms of MTOM variation, between OBS architectures when the integration level is increased by enhancing the employed workflow. This means that using a workflow where the OBS discipline is not fully integrated, the possible advantages obtained from OBS electrification is not completely captured. Comparing the results of the workflow n.1 where the OBS discipline is not integrated with the results of the other workflows, it is possible to obtain the diagram shown in Figure 15. Analyzing the diagram, the following points can be observed:

- Increasing the integration level, a variation of about 1% of MTOM can be observed when the results of workflow n.1 are compared with those of workflow n.4. 1% of MTOM represents about the 40% of the actual MTOM variation due to different OBS architecture. This means that using the workflow n.1 an error of about 40% could be expected.
- For conventional OBS architecture, the error is quite small changing the integration level. It could be due to the assumptions considered in the other disciplinary tools that are already set for conventional systems. As a consequence, and looking the variation for the other architectures, to correctly evaluate innovative systems, a workflow with higher level of integration is necessary.
- Among the integrated disciplines, the SFC variation due to the OBS power offtakes represents an important improvement in the results, as shown on Figure 15 for workflow n.3. This is particularly true for MEA2 architecture that in workflow n.2 produces the same effect of the conventional configuration.
- Finally, the aircraft redesign, discipline added in workflow n.4, is the greater contributor to the correct integration of the OBS design. The airframe and geometry redesign produce a notable effect on all the other disciplines involved (aircraft performance and engine design). This time, the enhancement added with workflow n.4 improve the results of MEA1 and AEA architectures that entail the greater mass reduction that can be correctly inherited by the other aircraft components by means of the aircraft synthesis.



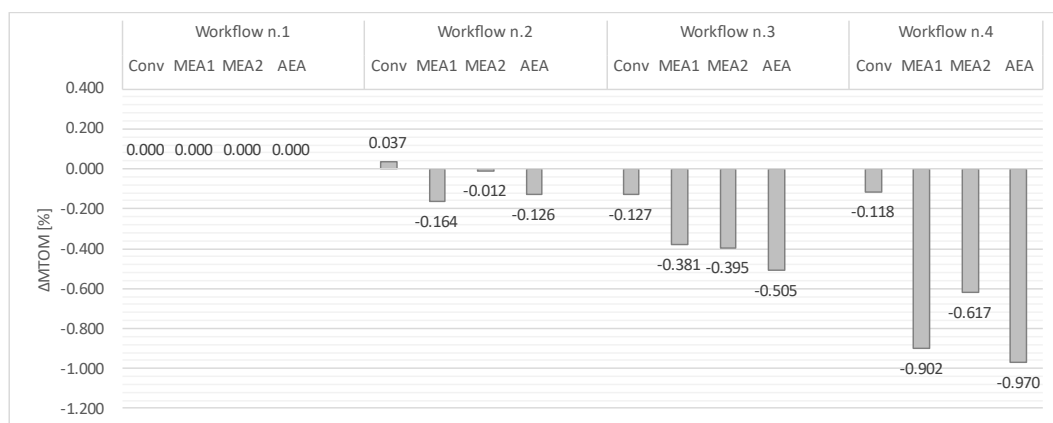
498

499

Figure 14. Different assessment of OBS architectures using the four workflows under study having as reference the conventional architecture

500

501



502

Figure 15. Different assessment of OBS architectures using the four workflows under study having as reference workflow n.1

503

5. Conclusions

504

The present paper shows the importance of increasing the integration of the OBS design with the other disciplines, especially when a comparison among different systems architectures is needed. Four workflows, with an increasing level of OBS integration, are proposed and tested. Each workflow has been utilized to design a small regional aircraft, with fixed TLARs, and with four OBS architectures with different level of electrification. The results demonstrate that the OBS design discipline is mainly connected with the other by two parameters, the systems mass and the system power requirement. The systems mass parameter should be captured by all the design disciplines of a MDO workflow (e.g. engine and airframe design, mission performance). The second parameter, the systems power requirement, should be taken into account by the engine design considering the important influence on the performance of the propulsion system. The power requirement together with its influence on engine efficiency produces, in turns, an effect on fuel mass and hence on the mass of all aircraft components.

505

506

507

508

509

510

511

512

513

514

515

516

517

Comparing the results of the different workflows in terms of aircraft MTOM, an error of about 40% on OBS architectures assessment has been found when the OBS discipline is not fully integrated with the others. This happens mainly when electrified OBS architecture are considered. A lower error is encountered for the conventional system architecture since the workflow tools are inherently set for it. Therefore, having the electrified architectures new influences on the other aircraft components and performance, to correctly address them, it is necessary to deeply integrate the workflow disciplines to catch their mutual influences that cannot be assumed in the tools themselves.

518

519

520

521

522

523

524

525

Another interesting result of the present paper concerns the systems electrification. All electrified architectures provide advantages in terms of mass and fuel saving. In particular, the removal of the HPGDS greatly reduce the OBS mass avoiding the installation of hydraulic pipes, fluid and dedicated equipment not utilized by other systems. On the contrary, the electrification produces a synergic effect among systems and the rise of the EPGDS mass can be dampened using high voltage technology. A reduction of MTOM of 2.6% is expected when those technology improvements are implemented as in MEA1 architecture. Another important step for OBS electrification is the use of the bleed-less technology. For the aircraft category here analyzed, this does not produce an important mass improvement, but a more substantial fuel saving. The AEA architecture entails a reduction of MTOM of 2.4% but a reduction of fuel burnt of 2.8% (0.8% higher than MEA1).

Finally, possible improvements can be evaluated in future analyses. A secondary influence of the OBS to the other design disciplines is related to the systems volume and the need of air flow for temperature control. The OBS volume has an effect on the aircraft shape (e.g. landing gear and actuators fairings) and it changes accordingly to the technology selected for each component. This would be a further integration in order to evaluate a difference in aircraft drag. In this way, the air intakes needed by the OBS also differ with the electrification level and they have an additional influence on aircraft drag.

Author Contributions: All authors contributed equally to writing this article. They teamed up to design the presented models and the associated computational framework, to analyze the data, to carry out the implementation, and finally to perform the calculation examples. All authors have read and agreed to the published version of the manuscript.

Funding: This research was funded by European Union Horizon 2020 Programme, CINEA agency, grant number 815122, under the acronym AGILE 4.0 (Towards cyber-physical collaborative aircraft development) research project.

Acknowledgments: The authors want to thank the whole AGILE 4.0 consortium for the support provided on the technologies developed and used in this research.

Conflicts of Interest: The authors declare no conflict of interest. The funders had no role in the design of the study; in the collection, analyses, or interpretation of data; in the writing of the manuscript, or in the decision to publish the results.

Abbreviations

The following abbreviations are used in this manuscript:

ACM	=	Air Cycle Machine	559
AEA	=	All Electric Aircraft	560
ECS	=	Environmental Control System	561
EDP	=	Engine Driven Pump	562
EHA	=	Electro Hydrostatic Actuator	563
EPGDS	=	Electric Power Generation and Distribution System	564
FCS	=	Flight Control System	565
HPGDS	=	Hydraulic Power Generation and Distribution System	566
IPS	=	Ice Protection System	567
MDAO	=	Multidisciplinary Design Analysis and Optimization	568
MEA	=	More Electric Aircraft	569
MTOM	=	Maximum Take Off Mass	570
OAD	=	Overall Aircraft Design	571
OBS	=	On-Board Systems	572
OEM	=	Operating Empty Mass	573

PPGDS	= Pneumatic Power Generation and Distribution System	574
PPDU	= Primary Power Distribution Unit	575
SFC	= Specific Fuel Consumption	576
SPDU	= Secondary Power Distribution Unit	577
TLARs	= Top Level Aircraft Requirements	578
TOFL	= Take Off Field Length	579
L_E	= Level of electrification [-]	580
P_E	= Total electric power generated [W]	581
P_T	= Total non-propulsive power generated [W]	582

References

- Cronin, M. J. All-Electric vs Conventional Aircraft: The Production/Operational Aspects., *J. of Air.* **1983**, *20*, 481-486. 584
- Sinnet, M. 787 No-Bleed Systems: Saving Fuel and Enhancing Operational Efficiencies. *Aero Quarterly* **2007**, QTR_04 | 07, 06-11. 585
- Della Vecchia, P., Stingo, L., Nicolosi, F., De Marco, A., Cerino, G., Ciampa, P.D., Prakasha, P.S., Fioriti, M., Zhang, M., Mirzoyan, A. and Aigner, B., 2018. Advanced turboprop multidisciplinary design and optimization within AGILE project. In 2018 Aviation Technology, Integration, and Operations Conference (p. 3205). 586
- Jones, R. I. The more electric aircraft—assessing the benefits. *J. of Aero. Eng.* **2002**, *216*, 259-269. 589
- Fioriti, M., Vercella, V., & Viola, N. (2018). Cost-Estimating Model for Aircraft Maintenance. *AIAA Journal of Aircraft*, *55*(4), 1564-1575. doi:10.2514/1.C034664 590
- Chiesa, S., & Fioriti, M. (2015). UAV logistic support definition. In *Handbook of Unmanned Aerial Vehicles* (pp. 2565-2600). Springer Netherlands. doi:10.1007/978-90-481-9707-1_79 592
- Raymer, D. P. *Aircraft Design: A Conceptual Approach*; Publisher: AIAA Education Series. Washington D.C, USA, 1992. 594
- Roskam, J. *Airplane Design*, 2nd ed.; Publisher: Roskam Aviation and Engineering Corporation Ottawa, Kansas, USA, 1989. 595
- Torenbeek, E. *Synthesis of Subsonic Airplane Design*, 1st ed; Publisher: Nijgh-Wolters-Noordhoff, Rotterdam, the Netherlands, 1976. 596
- Martins Pires, R. M.; Lajux, V.; Fielding, J. P.; Methodology for the Design and Evaluation of Wing Leading Edge and Trailing Edge Devices. *Proceedings of International Congress of the Aeronautical Sciences*, 2006, Hamburg, Germany. 599
- Sobieszczanski-Sobieski, J. Multidisciplinary Design Optimization: An Emerging New Engineering Discipline. *Adv. in Struc. Opt.* **1995**, 483-496. 600
- Werner-Westphal, C.; Heinze, W.; Horst, P.. Multidisciplinary Integrated Preliminary Design Applied to Unconventional Aircraft Configuration. *J. of Air.* **2008**, *45*, 581-590. 602
- Allison, D. L.; Alyanak, E. J.; Shimmin, K. Aircraft system effects including propulsion and air cycle machine coupled interactions. 57th AIAA/ASCE/AHS/ASC Structures, Structural Dynamics, and Materials Conference, 2016, USA. 604
- Jeyaraj, A. K.; Tabesh, N.; Liscouet-Hanke, S. Connecting Model-based Systems Engineering and Multidisciplinary Design Analysis and Optimization for Aircraft System Architecting. *AIAA AVIATION 2021 FORUM*, 2021, USA. 606
- Chakraborty, I., & Mavris, D. N. (2016). Integrated Assessment of Aircraft and Novel Subsystem Architectures in Early Design. *AIAA SciTech.*, 2016, USA. 608
- Ciampa, P. D.; Nagel, B.; La Rocca, G. A MBSE Approach to MDAO Systems for the Development of Complex Products, *AIAA Aviation, Virtual*, 06/01/2020, 2020. 610
- EASA, Certification Specifications for Normal, Utility, Aerobatic and Commuter Category Aeroplanes CS-23, July 2012. 612
- Fioriti, M.; Boggero, L.; Prakasha, P.; Mirzoyan, A.; Aigner, B., Anisimov, K. Multidisciplinary aircraft integration within a collaborative and distributed design framework using the AGILE paradigm. *Pro. Aer. Sci.* **2020**, *119*, 1-14. 613
- Liersch, C.; Hepperle, M. A. A distributed toolbox for multidisciplinary preliminary aircraft design. *CEAS Aer. J.* **2011**, *2*, 57 - 68. 615
- Zill, T.; Böhnke, D.; Nagel, B. Preliminary Aircraft Design in a Collaborative Multidisciplinary Design Environment. 11th AIAA Aviation Technology, Integration and Operations Conference. Virginia Beach, USA, 2011. 617
- Moerland, E.; Pfeiffer, T.; Böhnke, D.; Jepsen, J.; Freund, S.; Liersch, C.; Hasan, Y. On the Design of a Strut-Braced Wing Configuration in a Collaborative Design Environment. *AIAA AVIATION Forum*. Denver, USA, 2017. 619
- Torenbeek, E. *Synthesis of Subsonic Airplane Design*, 2nd ed.; Publisher: Nijgh-Wolters-Noordhoff, Rotterdam, the Netherlands, 1984. 621
- Roskam, J. *Airplane Design*, 1st ed.; Publisher: Roskam Aviation and Engineering Corporation Ottawa, Kansas, USA, 1985. 623
- Raymer, D. P., *Aircraft Design: A Conceptual Approach*, 1st ed.; Washington DC, USA: AIAA Education Series, 2012. 624
- Torenbeek, E. *Advanced Aircraft Design*, 1st ed.; the Netherlands: Wiley Aerospace Series, 2013. 625
- Jenkinson, L. R.; Simpkin, P.; Rhodes, D. *Civil Jet Aircraft Design*. Butterworth Heinemann, United Kingdom, 1999. 626
- Wells, D. P.; Horvath, B. L.; McCullers, L. A. *The Flight Optimization System - Weights Estimation Method*. NASA Langley Research Center. Virginia, USA, 2017. 627

-
28. Woehler, S.; Atanasov, G.; Silberhorn, D.; Fröhler, B.; Zill, T. *Preliminary Aircraft Design within a Multidisciplinary and Multifidelity Design Environment*, Aerospace Europe Conference, 25.-28. Feb. 2020, Bordeaux, Frankreich, 2020. 629
630
 29. Chiesa, S., Fioriti, M. and Viola, N., 2012. Methodology for an integrated definition of a System and its Subsystems: the case-study of an Airplane and its Subsystems. *Systems Engineering—Practice and Theory*, pp.1-26. 631
632
 30. Nicolosi, F.; De Marco, A.; Attanasio, L.; Della Vecchia P., Development of a Java-Based Framework for Aircraft Preliminary Design and Optimization. *J. Aerosp. Inf. Syst* **2016**, *13*, 234–242. 633
634
 31. De Marco, A; Trifari, V.; Nicolosi, F; Ruocco, M, A simulation-based performance analysis tool for aircraft design workflows. *Aerospace* **2020**, *7*, 1-32. 635
636
 32. Trifari, V.; Ruocco, M.; Cusati, V.; Nicolosi, F.; De Marco, A. Java Framework for Parametric Aircraft Design—Ground Performance. *Aircr. Eng. Aerosp. Technol.* **2017**, 89. 637
638
 33. Trifari, V. Development of a Multi-Disciplinary Analysis and Optimization framework and applications for innovative efficient regional aircraft, PhD thesis **2020**, 32 cycle, University of Naples Federico II. 639
640
641